arXiv:1602.06060v1 [nucl-th] 19 Feb 2016

Electromagnetic and Weak Nuclear Structure Functions $F_{1,2}(x, Q^2)$ in the Intermediate Region of Q^2

H. Haider[1], F. Zaidi[1], M. Sajjad Athar[1], S. K. Singh[1], I. Ruiz Simo[2]

[1]*Department of Physics, Aligarh Muslim University, Aligarh - 202 002, India,* [2]*Departamento de Física Atómica, Molecular y Nuclear, and Instituto de Física Teórica y Computacional Carlos I, Universidad de Granada, Granada 18071, Spain*

E-mail: huma.haider8@gmail.com

(Received January 19, 2016)

We have studied nuclear structure functions $F_{1A}(x, Q^2)$ and $F_{2A}(x, Q^2)$ for electromagnetic and weak processes in the region of $1\ GeV^2 < Q^2 < 8\ GeV^2$. The nuclear medium effects arising due to Fermi motion, binding energy, nucleon correlations, mesonic contributions and shadowing effects are taken into account using a many body field theoretical approach. The calculations are performed in a local density approximation using a relativistic nucleon spectral function. The results are compared with the available experimental data. Implications of nuclear medium effects on the validity of Callan-Gross relation are also discussed.

KEYWORDS: nuclear medium effect, structure functions, deep inelastic scattering, Callan-Gross relation

1. Introduction

Recently a better understanding of nuclear medium effects in the deep inelastic scattering region both in electromagnetic(EM) and weak(Weak) interaction induced processes has been emphasized due to the fact that experiments are being performed using electron beam at JLab [1] and neutrino/antineutrino beam at the Fermi Lab. The experiments are being performed using several nuclear targets. The differential and total scattering cross sections are expressed in terms of $F_{1A}^{EM}(x, Q^2)$ and $F_{2A}^{EM}(x, Q^2)$ structure functions for electromagnetic processes and for weak interaction induced processes in terms of $F_{1A}^{Weak}(x, Q^2)$, $F_{2A}^{Weak}(x, Q^2)$ and $F_{3A}^{Weak}(x, Q^2)$ structure functions. We have studied nuclear medium effects arising due to Fermi motion, binding energy, nucleon correlations, mesonic contributions and shadowing effects in these structure functions, in a many body field theoretical approach and the calculations are performed in a local density approximation using a relativistic nucleon spectral function. The details of the present formalism are given in Ref. [2]. In this paper, we have compared $F_{1A}^{EM}(x, Q^2)$ vs $F_{1A}^{Weak}(x, Q^2)$, and $F_{2A}^{EM}(x, Q^2)$ vs $F_{2A}^{Weak}(x, Q^2)$ structure functions. The results for the ratio $\frac{2xF_{1A}(x,Q^2)}{F_{2A}(x,Q^2)}$ with nuclear medium effects in carbon has also been presented. The results are also compared with some of the available experimental data. For completeness, we are presenting the formalism in brief.

2. Formalism

The double differential cross section for the reaction $\nu_l/\bar{\nu}_l(k)+N(p) \rightarrow l^-/l^+(k')+X(p')$, $l = e^-, \mu^-$, in the Lab frame is written as

$$\frac{d^2\sigma^N_{\nu,\bar{\nu}}}{d\Omega' dE'} = \frac{G_F^2}{(2\pi)^2}\,\frac{|\mathbf{k}'|}{|\mathbf{k}|}\left(\frac{m_W^2}{q^2-m_W^2}\right)^2 L^{\alpha\beta}_{\nu,\bar{\nu}}\,W^N_{\alpha\beta}\,, \tag{1}$$

where $L^{\alpha\beta}_{\nu,\bar{\nu}} = k^\alpha k'^\beta + k^\beta k'^\alpha - k.k' g^{\alpha\beta} \pm i\epsilon^{\alpha\beta\rho\sigma}k_\rho k'_\sigma$ is the leptonic tensor with (+ve)-ve sign for (anti)neutrino, and $W^N_{\alpha\beta}$ is the nucleon hadronic tensor expressed in terms of nucleon structure functions W^N_i; $i = 1-3$,

$$W^N_{\alpha\beta} = \left(\frac{q_\alpha q_\beta}{q^2} - g_{\alpha\beta}\right) W_1^N + \frac{1}{M_N^2}\left(p_\alpha - \frac{p.q}{q^2}\,q_\alpha\right)\left(p_\beta - \frac{p.q}{q^2}\,q_\beta\right)W_2^N - \frac{i}{2M_N^2}\epsilon_{\alpha\beta\rho\sigma}p^\rho q^\sigma W_3^N. \tag{2}$$

In a nuclear medium the expression for the cross section is written as

$$\frac{d^2\sigma^A_{\nu,\bar{\nu}}}{d\Omega' dE'} = \frac{G_F^2}{(2\pi)^2}\,\frac{|\mathbf{k}'|}{|\mathbf{k}|}\left(\frac{m_W^2}{q^2-m_W^2}\right)^2 L^{\alpha\beta}_{\nu,\bar{\nu}}\,W^A_{\alpha\beta}\,, \tag{3}$$

$W^A_{\alpha\beta}$ is the nuclear hadronic tensor defined in terms of nuclear structure functions W^A_i; $i = 1-3$,

$$W^A_{\alpha\beta} = \left(\frac{q_\alpha q_\beta}{q^2} - g_{\alpha\beta}\right) W_1^A + \frac{1}{M_A^2}\left(p_\alpha - \frac{p.q}{q^2}\,q_\alpha\right)\left(p_\beta - \frac{p.q}{q^2}\,q_\beta\right)W_2^A - \frac{i}{2M_A^2}\epsilon_{\alpha\beta\rho\sigma}p^\rho q^\sigma W_3^A \tag{4}$$

where M_A is mass of the target nucleus. The neutrino-nucleus cross sections are written in terms of neutrino self energy $\Sigma(k)$ in the nuclear medium, the expression for which is obtained as [2]:

$$\Sigma(k) = \frac{-iG_F}{\sqrt{2}}\frac{4}{m_\nu}\int\frac{d^4k'}{(2\pi)^4}\frac{1}{k'^2 - m_l^2 + i\epsilon}\left(\frac{m_W}{q^2-m_W^2}\right)^2 L_{\alpha\beta}\;\Pi^{\alpha\beta}(q)\,. \tag{5}$$

$\Pi^{\alpha\beta}(q)$ is the W-boson self energy in the nuclear medium which is given in terms of nucleon (G) and meson (D_j) propagators

$$\begin{aligned} -i\Pi^{\alpha\beta}(q) \;\;=\;\; & (-)\int\frac{d^4p}{(2\pi)^4}iG(p)\;\sum_X\sum_{s_p,s_i}\prod_{i=1}^{n}\int\frac{d^4p'_i}{(2\pi)^4}\prod_l iG_l(p'_l)\prod_j iD_j(p'_j) \\ & \times\left(\frac{-G_F m_W^2}{\sqrt{2}}\right)\langle X|J^\alpha|N\rangle\langle X|J^\beta|N\rangle^*(2\pi)^4\delta^4(q+p-\Sigma_{i=1}^n p'_i). \end{aligned} \tag{6}$$

Using the expression of W self-energy and neutrino self-energy in the expression of cross section one obtains [2]:

$$W^A_{\alpha\beta} = 4\int d^3r\int\frac{d^3p}{(2\pi)^3}\int_{-\infty}^{\mu}dp^0\,\frac{M}{E(\mathbf{p})}S_h(p^0,\mathbf{p},\rho(r))W^N_{\alpha\beta}(p,q), \tag{7}$$

where μ is the chemical potential. The hole spectral function S_h takes care of Fermi momentum, Pauli blocking, binding energy and nucleon correlations [3]. $W^N_i(x,Q^2)$ and $W^A_i(x,Q^2)$ are respectively redefined in terms of the dimensionless structure functions $F^N_i(x,Q^2)$ and $F^A_i(x,Q^2)$ through

$$MW^N_1(\nu,Q^2) \;\;=\;\; F^N_1(x,Q^2); \qquad M_A W^A_1(\nu,Q^2) = F^A_1(x,Q^2)$$

$$\nu W_2^N(\nu, Q^2) = F_2^N(x, Q^2); \qquad \nu_A W_2^A(\nu, Q^2) = F_2^A(x, Q^2)$$
$$\nu W_3^N(\nu, Q^2) = F_3^N(x, Q^2); \qquad \nu_A W_3^A(\nu, Q^2) = F_3^A(x, Q^2)$$

The nucleon structure functions are expressed in terms of parton distribution functions(PDFs). For the numerical calculations, we have used CTEQ6.6 [4] nucleon PDFs. The evaluations are performed both at the leading order(LO) and next-to-leading order(NLO). For electromagnetic interaction, we follow the same procedure, formalism for which is given in accompanying paper by Zaidi et al. [5] in this proceeding.

Expressing $W^N_{\alpha\beta}$ and $W^A_{\alpha\beta}$, in terms of F^N_i and F^A_i (i=1,2), we get [2]

$$F_{1\,A}^{EM/Weak}(x_A, Q^2) = 2\sum_{\tau=p,n} AM \int d^3r \int \frac{d^3p}{(2\pi)^3}\frac{M}{E(\mathbf{p})}\int_{-\infty}^{\mu} dp_0 S_h^{\tau}(p_0, \mathbf{p}, \rho^{\tau}(r)) \times \left[\frac{F_1^{EM/Weak,\tau}(x_N, Q^2)}{M} + \frac{{p_x}^2}{M^2}\frac{F_2^{EM/Weak,\tau}(x_N, Q^2)}{\nu}\right], \tag{8}$$

$$F_{2\,A}^{EM/Weak}(x_A, Q^2) = 2\sum_{\tau=p,n}\int d^3r \int \frac{d^3p}{(2\pi)^3}\frac{M}{E(\mathbf{p})}\int_{-\infty}^{\mu} dp_0 S_h^{\tau}(p_0, \mathbf{p}, \rho^{\tau}(r)) \times \left[\frac{Q^2}{q_z^2}\left(\frac{|\mathbf{p}|^2 - p_z^2}{2M^2}\right) + \frac{(p_0 - p_z\,\gamma)^2}{M^2}\left(\frac{p_z\,Q^2}{(p_0 - p_z\,\gamma)q_0 q_z} + 1\right)^2\right] \times \left(\frac{M}{p_0 - p_z\,\gamma}\right) F_2^{EM/Weak,\tau}(x, Q^2), \tag{9}$$

where $\gamma = \frac{q_z}{q_0} = \sqrt{1 + \frac{4M^2x^2}{Q^2}}$. The mesonic (pion and rho) cloud contributions are taken into account following the same procedure as for the nucleon, except the fact that now instead of nucleon spectral function, we use meson propagator to describe the meson propagation in the nuclear medium. For this also, we have used microscopic approach by making use of the imaginary part of the meson propagators instead of spectral function, and obtain $F^A_{2,\pi}(x)$ [3] as

$$F_{2,A,\pi}^{EM/Weak}(x_\pi, Q^2) = -6\int d^3r \int \frac{d^4p}{(2\pi)^4}\,\theta(p_0)\,\delta ImD(p)\,2m_\pi\left(\frac{m_\pi}{p_0 - p_z\,\gamma}\right)\times \left[\frac{Q^2}{q_z^2}\left(\frac{|\mathbf{p}|^2 - p_z^2}{2m_\pi^2}\right) + \frac{(p_0 - p_z\gamma)^2}{m_\pi^2}\left(\frac{p_z\,Q^2}{(p_0 - p_z\gamma)q_0 q_z} + 1\right)^2\right] F_{2,\pi}^{EM/Weak}(x_\pi) \tag{10}$$

where $x_\pi = -\frac{Q^2}{2p\cdot q}$ and $D(p)$ is the pion propagator in the nuclear medium given by

$$D(p) = [{p_0}^2 - \mathbf{p}^2 - m_\pi^2 - \Pi_\pi(p_0, \mathbf{p})]^{-1}, \tag{11}$$

where

$$\Pi_\pi = \frac{f^2/m_\pi^2 F^2(p)\mathbf{p}^2\Pi^*}{1 - f^2/m_\pi^2 V_L'\Pi^*}. \tag{12}$$

Here, $F(p) = (\Lambda^2 - m_\pi^2)/(\Lambda^2 + \mathbf{p}^2)$ is the πNN form factor, Λ=1 GeV, $f = 1.01$, V_L' is the longitudinal part of the spin-isospin interaction and Π^* is the irreducible pion self energy containing the contribution from particle - hole and delta - hole excitations. For the meson PDFs we have used the

parameterization of Gluck et al. [6]. Similarly, the contribution of the ρ-meson cloud to the structure function is taken into account [3]

$$F_{2,A,\rho}^{EM/Weak}(x_\rho, Q^2) = -12 \int d^3r \int \frac{d^4p}{(2\pi)^4}\, \theta(p_0)\, \delta ImD(p)\, 2m_\rho \left(\frac{m_\rho}{p_0 - p_z\,\gamma}\right) \times \left[\frac{Q^2}{q_z^2}\left(\frac{|\mathbf{p}|^2 - p_z^2}{2m_\rho^2}\right) + \frac{(p_0 - p_z\,\gamma)^2}{m_\rho^2}\left(\frac{p_z\,Q^2}{(p_0 - p_z\,\gamma)q_0 q_z} + 1\right)^2\right] F_{2,\rho}^{EM/Weak}(x_\rho) \quad (13)$$

where $x_\rho = -\frac{Q^2}{2p\cdot q}$ and $D_\rho(p)$ is now the ρ-meson propagator in the medium given by:

$$D_\rho(p) = [{p_0}^2 - \mathbf{p}^2 - m_\rho^2 - \Pi_\rho^*(p_0, \mathbf{p})]^{-1}\,, \quad (14)$$

where

$$\Pi_\rho^* = \frac{f^2/m_\rho^2 C_\rho F_\rho^2(p)\mathbf{p}^2\Pi^*}{1 - f^2/m_\rho^2 V_T'\Pi^*}\,. \quad (15)$$

In Eq.15, V_T' is the transverse part of the spin-isospin interaction, $C_\rho = 3.94$, $F_\rho(p) = (\Lambda_\rho^2 - m_\rho^2)/(\Lambda_\rho^2 + \mathbf{p}^2)$ is the ρNN form factor, Λ_ρ=1 GeV, $f = 1.01$, and Π^* is the irreducible rho self energy which contains the contribution of particle - hole and delta - hole excitations. We have used the same PDFs for the ρ meson as for the pions [6].

We have also included shadowing effect following the works of Kulagin and Petti [7]. For the shadowing effect which is due to the constructive interference of amplitudes arising from the multiple scattering of quarks inside the nucleus, Glauber-Gribov multiple scattering theory has been used. Shadowing effect is a low x and low Q^2 phenomenon which becomes negligible for high x. We label the results of spectral function(SF) with meson cloud contribution and shadowing effect, as the results obtained with full prescription(Total).

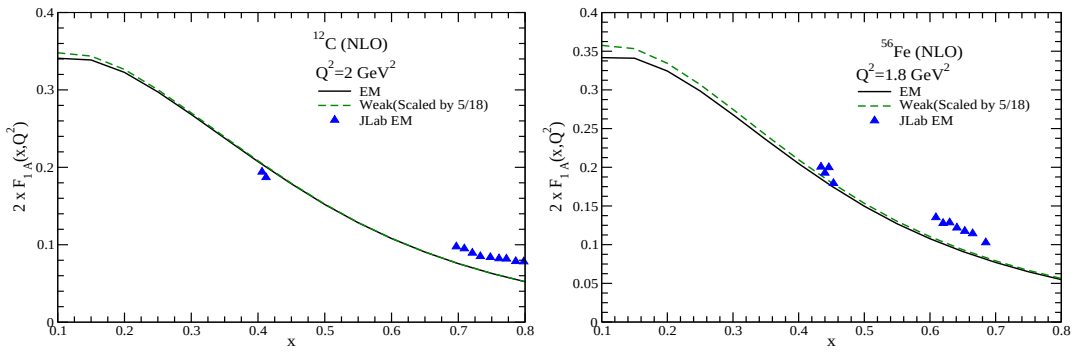

Fig. 1. Results for the $2xF_{1\,A}(x, Q^2)$ in $(A =)^{12}C$ and ^{56}Fe nuclei at NLO with full prescription. The experimental points are JLab data [1].

3. Results

In Fig.1, the results for $2xF_{1A}(x, Q^2)$ are shown for electromagnetic and weak interactions in carbon and iron nuclei at a fixed Q^2 with full prescription for nuclear medium effect. The results for $2xF_{1A}^{EM}(x, Q^2)$ are compared with the JLab [1] data. We found that the present results are consistent with the experimental data. From the figure, one may observe that at low x, EM structure function

is slightly different from weak structure function which is about 1 – 2% for carbon. This difference increases with the increase in mass number, for example, in iron it is ~ 4% at x=0.1. This difference is significant at low x and becomes almost negligible for high x. This difference has also been found in the free nucleon case which shows a different distribution of sea quarks for electromagnetic and weak interaction processes. Moreover, the difference in the case of nuclear target becomes a bit larger from the free nucleon case due to nuclear medium and nonisoscalarity effects.

Similar is the observation for $F_{2A}(x, Q^2)$ in the electromagnetic as well as weak structure functions as may be observed in Fig.2. In Fig.3 (left panel), we have shown the effect of mesonic cloud

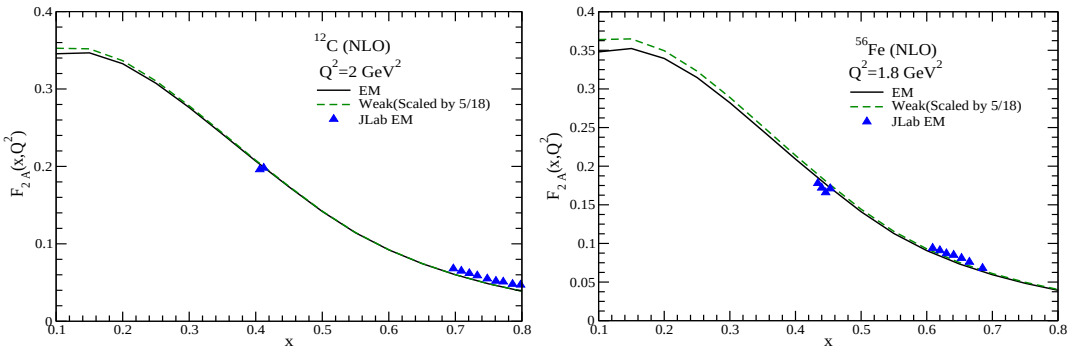

Fig. 2. Results for $F_{2\,A}(x, Q^2)$ in $(A =)^{12}C$ and ^{56}Fe nuclei at NLO with full prescription. The experimental points are JLab data [1].

contribution and shadowing effect on the electromagnetic structure functions $F_{1A}(x, Q^2)$ and $F_{2A}(x, Q^2)$. For this, we are presenting the results using the expression $r_i = \frac{F_i^{Modified}(x,Q^2) - F_i^{SF}(x,Q^2)}{F_i^{Modified}(x,Q^2)}$, (i=1,2), for ^{56}Fe at $Q^2 = 5\ GeV^2$, where $F_i^{SF}(x, Q^2)$ stands for the results obtained for the nuclear structure functions using the spectral function(SF) only while $F_i^{Modified}(x, Q^2)$ is the result obtained when we include **(i)** mesonic$(\pi + \rho)$ cloud contribution, **(ii)** mesonic$(\pi + \rho)$ cloud contribution and shadowing effect. Mesonic cloud contribution is effective in the intermediate region of x $(x \leq 0.6)$. The inclusion of shadowing effect hardly changes this ratio.

Furthermore, the effect of mesonic contributions is to increase $2xF_{1A}(x, Q^2)$ and $F_{2A}(x, Q^2)$. The increase is larger at small $x(x < 0.3)$, for example 20% at $x = 0.2$, 12% at $x = 0.3$ and smaller at high $x(x > 0.5)$, for example ~ 2% at $x = 0.5$. The increment in the results of $F_{2A}(x, Q^2)$ is more than in the results of $2xF_{1A}(x, Q^2)$ over an entire range of x. We have also studied this ratio in the case of weak interaction and found that the results almost overlap with the results obtained for EM interaction.

It may be observed that when shadowing effects are included there is net reduction in the result. This is because the shadowing and the mesonic effects tend to cancel each other specially in the region of small $x(x < 0.2)$, where shadowing is important.

In the right panel of Fig.3, we have presented the results for EM and weak structure functions $F_{2A}(x, Q^2)$ in iron at $Q^2 = 6\ GeV^2$ and compared them with some of the experimental data [8–14] available for $F_{2A}^{EM}(x, Q^2)$ and $F_{2A}^{Weak}(x, Q^2)$. One may observe that theoretically $F_{2A}^{EM}(x, Q^2)$ lies below $F_{2A}^{Weak}(x, Q^2)$ over the entire region of x. Furthermore, we observe that explicitly our model in agreement with the experimental data of CCFR [8], EMC139 [10, 11], EMC140 [12] and NuTeV [14] experiments.

To quantify our results in Fig.4, we present the results for the ratio of $\frac{2xF_{1A}(x,Q^2)}{F_{2A}(x,Q^2)}$ in carbon and compare it with the JLab data [1]. We have found that the ratio of $\frac{2xF_{1A}(x,Q^2)}{F_{2A}(x,Q^2)}$ is different than

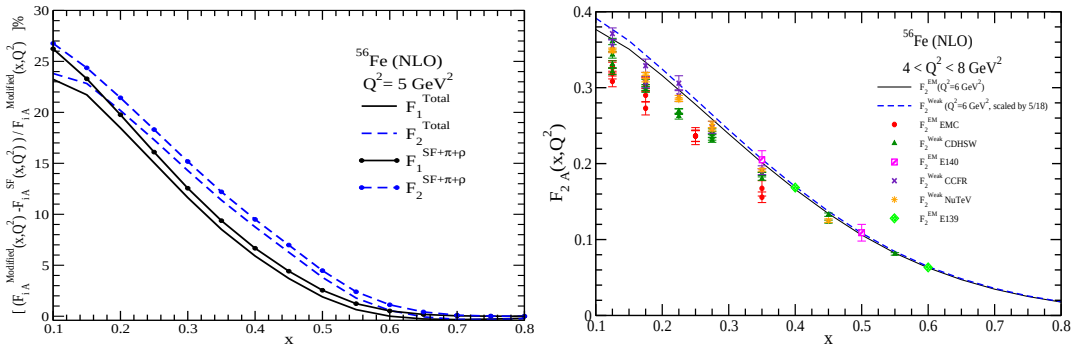

Fig. 3. **Left panel:** r_i vs x in $(A =)^{56}Fe$ at $Q^2 = 5\ GeV^2$ for EM interaction at NLO; **Right panel:** Results for $F_{2\,A}(x, Q^2)$ in iron for EM and weak interactions at NLO with full prescription. The experimental points are data from Refs. [8–14]. It may be noted that the experimental data points lying below the theoretical curves are from the older experiments which have measured $F_{2\,A}^{EM}(x, Q^2)$ [13] and $F_{2\,A}^{Weak}(x, Q^2)$ [9].

unity, i.e. the results presented here give a microscopic description of deviation from Callan-Gross relation($\frac{2xF_{1A}(x,Q^2)}{F_{2A}(x,Q^2)} = 1$) due to nuclear medium effects. From the figure, one may observe that the ratio of EM and weak structure functions overlap each other. It would be interesting to make similar studies in the case of MINERvA experiment.

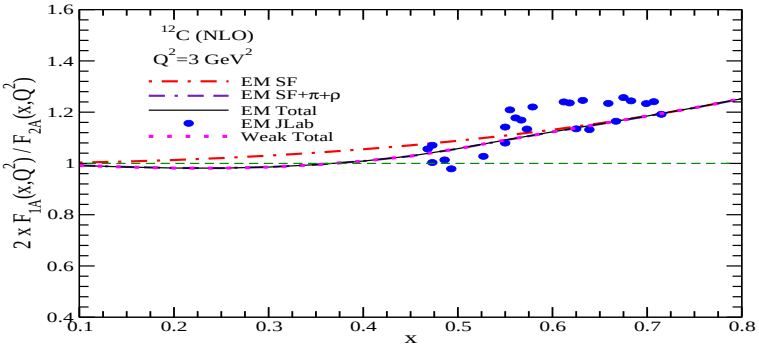

Fig. 4. Ratio of structure functions showing the violation of Callan-Gross relation at nuclear level. The experimental points are JLab data [1]. Dashed line corresponds to the Callan-Gross relation $\frac{2xF_{1A}(x,Q^2)}{F_{2A}(x,Q^2)} = 1$.

References

[1] V. Mamyan, arXiv:1202.1457 [nucl-ex].

[2] H. Haider, F. Zaidi, M. Sajjad Athar, S. K. Singh and I. Ruiz Simo, Nucl. Phys. A **943** (2015) 58, H. Haider, I. R. Simo, M. S. Athar and M. J. V. Vacas, Phys. Rev. C **84** (2011) 054610, M. Sajjad Athar, I. Ruiz Simo and M. J. Vicente Vacas, Nucl. Phys. A **857** (2011)29.

[3] E. Marco, E. Oset and P. Fernandez de Cordoba, Nucl. Phys. A **611**, (1996) 484.

[4] Pavel M. Nadolsky et al., Phys. Rev. D **78** (2008) 013004; http://hep.pa.msu.edu/cteq/public.

[5] F. Zaidi, H. Haider, M. Sajjad Athar, S. K. Singh and I. Ruiz Simo, in this Proceeding.

[6] M. Gluck, E. Reya and A. Vogt, Z. Phys. C **53** (1992) 651.

[7] S. A. Kulagin and R. Petti, Phys. Rev. D **76** (2007) 094023.

[8] E. Oltman *et al.*, Z. Phys. C **53** (1992) 51.

[9] J. P. Berge *et al.*, Z. Phys. C **49** (1991) 187.

[10] L.W. Whitlow, **SLAC-357** Ph.D. Thesis.
[11] O. Hen, D. W. Higinbotham, G. A. Miller, E. Piasetzky and L. B. Weinstein, Int. J. Mod. Phys. E **22** (2013) 1330017.
[12] S. Dasu *et al.*, Phys. Rev. D **49** (1994) 5641.
[13] J. J. Aubert *et al.*, Nucl. Phys. B **272** (1986) 158.
[14] M. Tzanov *et al.* , Phys. Rev. D **74** (2006) 012008.